The Circular Economy Challenge: Re-use of processing granite wastes for REEs-recovery: preliminary results.

Silvia Gioiello[1], Licia Santoro[1], Alberto Cazzaniga[2]
[1]Department of Earth Sciences, University of Torino, Italy
[2]Minerali Industriali S.r.l., Italy

Abstract. Chemical and minero-petrographic analyses by ICP-MS, XRPD, and SEM-EDS have been performed on scraps from the industrial processing of granite. The work aims to study the optimization of industrial processes by re-using the feldspar-treated waste material to recover Critical Raw Materials in the view of economic circularity and sustainable mining. The material used for this work derives from Montorfano quarry wastes (Piemonte, Italy). The ICP-MS analyses on the 1.2 to 0.1 mm fraction discarded after magnetic separation of granitic material for pure feldspar production show enrichment in Rare Earth Elements (REEs), mainly Ce, La, Nd, and Y. The XRPD and SEM-EDS analyses indicate that monazite, allanite, and xenotime are the main REE-bearing minerals, commonly locked within phyllosilicates. The results suggest that a further grinding on the unprocessed material is probably required to enhance particle liberation. Comminution to a particle size smaller than 0.1 mm, will lead to a more effective concentration of REEs minerals during magnetic separation.

1 Introduction

The growing economic importance and high supply risk make the availability of Critical Raw Materials (CRMs) a crucial issue for the European Union, which translates into the need to promote their exploration and recovery optimization to meet the foreseeable increase in demand. Most of these materials are essential for transitioning from the traditional energy system to a more sustainable one. However, domestic production is severely limited, resulting in a strong dependence on imports and uncertain access to resources. The present study focuses particularly on Rare Earth Elements (REEs), mainly used to manufacture components for high-tech and green technologies applications (European Commission, 2020a, b, c). Currently, China holds the monopoly on REEs production.

Moreover, mineral processing to recover such materials still represents a considerable challenge. Re-processing and re-use from quarry and mining wastes represent a good option to face the supply risk, leading to diversification of the supply chain and likely enhancement of domestic supply. In light of the above, this work aims to assess the viability of REEs recovery from mineral-processing industrial wastes, hence favoring a possible valorization and sustainable management of the processing scraps through their re-use in the frame of the Circular Economy.

The object of this research is a quarry disposal site located in the Lake District of the Verbano-Cusio-Ossola area (Piedmont, Italy), on the southern slope of the Montorfano massif (Figure 1a), where granite bodies were quarried as dimension stones for ornamental purposes, producing a huge volume of waste material. Such material is presently exploited to recover feldspar for ceramic and glass industries. The Montorfano pluton is intruded into gneissic rocks of the *Scisti dei Laghi* subunit, belonging to the *Serie dei Laghi* unit (Figure 1b). It is part of a NE-SW elongated batholith composed of many plutons occurring from the Biella area to the western shore of Lago Maggiore (Boriani et al. 1988).

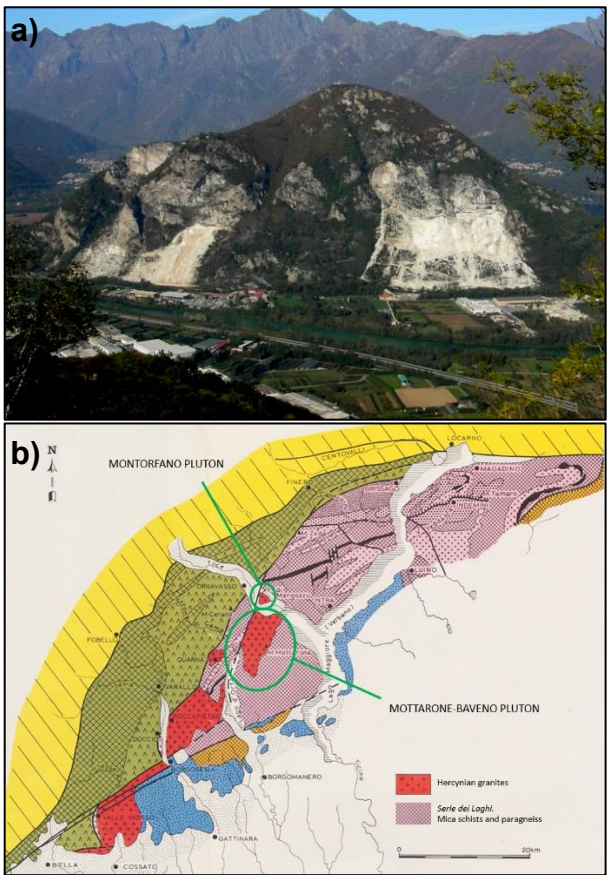

Figure 1. a Granite quarries on the southern side of Montorfano massif (Dino et al., 2012). **b** Tectonic sketch map of a portion of the central-southern Alps (Piedmont, Italy) and location of Montorfano and Mottarone-Baveno granitic plutons into *Serie dei Laghi* unit. Adapted from 1:50.000 geological map of the Verbania area (Boriani et al. 1977).

The pluton is a medium-grain white granite, whose mineralogical assemblage consists primarily of

plagioclase, quartz, K-feldspar, and biotite, including typical accessory minerals such as apatite, zircon, and allanite (Boriani et al. 1988). The occurrence of allanite-(Ce), together with other REEs-bearing minerals (e.g., Y-Sc-REEs-silicates, Y-REEs phosphates and Nb-Ta-Y-REEs oxides) has already been described in previous studies on the niobium-yttrium-fluorine (NYF) granitic pegmatite at Baveno (Guastoni et al. 2017).

A key purpose of the study was to evaluate the concentration process of ore minerals during the granite waste treatment aimed at feldspar production, performing detailed mineralogical and geochemical analyses on milled samples coming from different processing stages, as described in the following paragraph.

2 Methodology

Granite waste rock samples were collected in the Montorfano quarry and subsequently prepared and analyzed to define the behavior of REEs minerals in different types of concentrates resulting from industrial processing. All samples were crushed and ground in appropriate mills to achieve a grain size between 0.1 and 1.2 mm and then subjected to two different steps of magnetic separation, thus replicating the method used to obtain a pure feldspar concentrate. This process produces a “waste” magnetic fraction. The first separation step was applied on unprocessed material with grain size between 0.1 and 1.2 mm using a current of 2.5 Amp. Subsequently, the magnetic concentrate was sieved, and a second step was carried out on grain size of 0.1-0.6 mm using 2.5 Amp.

Wet chemical analyses by Inductively Coupled Plasma Mass Spectrometry (ICP-MS) were performed by ALS Laboratories on both the unprocessed material and the magnetic fraction for a large number of elements, including REEs (Sc, Ce, La, Nd, Sm, Pr, Eu, Dy, Er, Y, Gd, Ho, Lu, Tb, Tm and Yb) and other critical metals (e.g., Nb, Ta). Furthermore, the magnetic concentrates were investigated in terms of mineralogical and chemical composition through qualitative and quantitative analyses. Particularly, X-Ray Powder Diffraction (XRPD) analyses were carried out at the Minerali Industriali Engineering’s central laboratory to characterise the material. The acquisitions were carried out by using a Siemens D5000 Diffraktometer, operating at 40 kV, 40 mA, divergence slit 1, antiscatter slit 1, rotation 30, start 4 and stop 70. SEM-EDS analyses were carried out with a JEOL IT300LV Scanning Electron Microscope at the Department of Earth Sciences, University of Torino. The instrument was equipped with an energy dispersive spectrometry (EDS) Energy 200 system and an SDD X-Act3 detector (Oxford Inca Energy). Operating conditions were: 20 kV accelerating voltage, 5 nA probe current, 30 s counting time. SEM data were acquired and processed using the AzTec software (Oxford Instrument), version 6.0. In detail, microanalyses were acquired by using AzTec point ID suite. The use of SEM-EDS was combined with Automated Mineralogy (AM) analytical systems using a specific software package for data processing and automation (i.e., AztecFeature), which provides detailed particle analyses to be classified on the morphology and on the chemistry and combination of the two.

3 Results

Preliminary results described below refer to a representative sample indicated as *SNG*, which consists of a magnetic concentrate resulting from the first separation step, sieved to a grain size greater than 0.6 mm.

3.1 Wet chemical analyses (ICP-MS)

As shown in Table 1, chemical analysis on samples from different processing stages highlights a REEs enrichment in the magnetic concentrate compared to unprocessed material, particularly on the course fraction obtained from the first separation step. Light REEs (from Sc to Eu) are generally more abundant than heavy REEs (from Dy to Yb), and the highest values, are found for Ce, La and Nd. In addition, there is an increase in P from the unprocessed material to the magnetic fraction coinciding with the trend in REEs concentrations.

		TQ	SNG	SNS			TQ	SNG	SNS
Sc	ppm	8.6	55.3	32.9	**Dy**	ppm	4.86	22.2	12.45
Ce	ppm	89.9	434	256	**Er**	ppm	2.25	9.78	5.53
La	ppm	42	197	118	**Y**	ppm	22.8	99	64.3
Nd	ppm	40.5	198.5	125	**Gd**	ppm	6.76	32	17.9
Sm	ppm	8.34	39.2	23.3	**Ho**	ppm	0.86	3.82	2.19
Pr	ppm	10.8	51.9	32.5	**Lu**	ppm	0.28	1.13	0.69
Eu	ppm	0.77	1	0.82	**Tb**	ppm	0.92	4.24	2.28
					Tm	ppm	0.3	1.28	0.79
P	ppm	280	1460	700	**Yb**	ppm	1.91	8	4.95

Table 1. ICP-MS results for REEs and P. (TQ = unprocessed material; SNG = magnetic fraction >0.6 mm, 1st separation step) SNS = magnetic fraction <0.6 mm, 2nd separation step).

3.2 Mineralogy and petrography (XRPD/SEM-EDS)

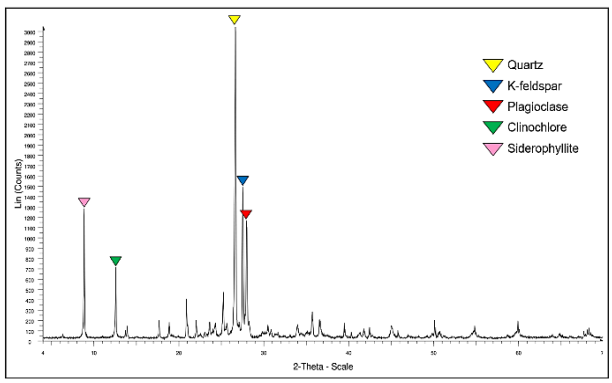

Figure 2. XRPD pattern showing prevailing gangue minerals in the coarse magnetic fraction (SNG sample).

Mineralogical characterization by XRPD helped identify the dominant gangue minerals in the SNG sample, represented by quartz, K-feldspar, plagioclase, clinochlore, and mica group minerals (e.g., siderophyllite), as shown in Figure 2. Peaks representative of REEs-minerals in the diffractogram are absent due to their concentrations falling below the instrument's detection limit.

Backscatter Electron (BSE) images and EDS on target minerals are presented respectively in Figure 3 and Table 2. The most common REEs mineral is monazite-(Ce), in agreement with the high P concentration of ICP-MS analyses (Table 1). Monazite locally shows tiny inclusions of thorite. Additionally, xenotime-(Y) and allanite (light grey) grains were spotted. REEs-bearing minerals seem generally associated with phyllosilicates (e.g., biotite, annite, siderophyllite, clinochlore) also observed on the XRPD pattern but are characterized by far smaller grain size. However, allanite has a larger grain size than monazite and xenotime. Zircon and ilmenite, often Nb-bearing, were also detected.

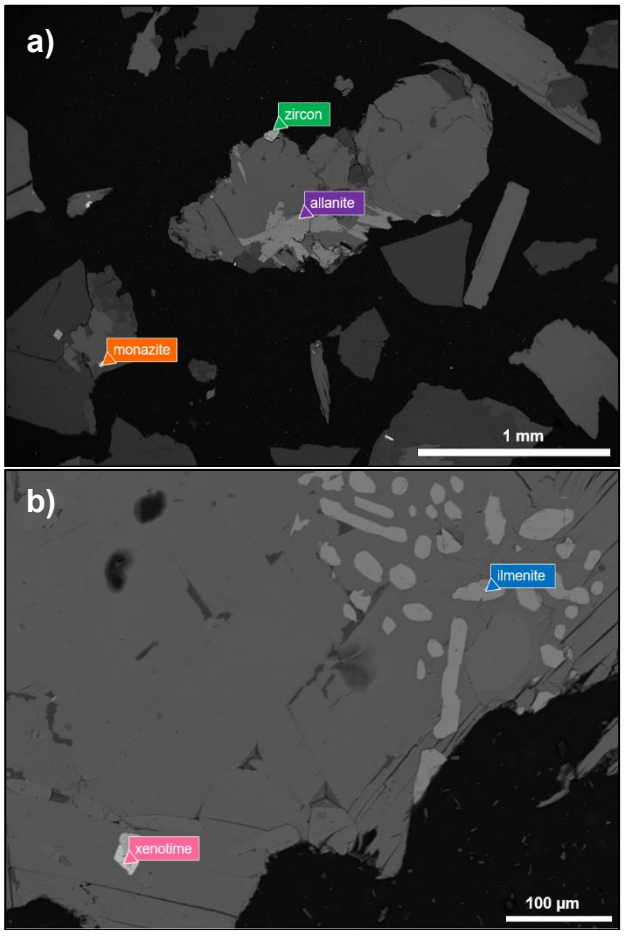

Figure 3. BSE images of selected areas on SNG sample, showing target minerals: **a** zircon (green, Spectrum 24), allanite (purple, Spectrum 25), monazite (orange, Spectrum 32) and **b** xenotime (pink, Spectrum 23), ilmenite (blue, Spectrum 22).

Monazite

	Spectrum 26 (normalised)				Spectrum 32 (normalised)			
	Oxide	Oxide %	Oxide % Sigma	Number of Ions	Oxide	Oxide %	Oxide % Sigma	Number of Ions
O				4				4
Si	SiO2	3.3	0.05	0.13	Al2O3	2.45	0.22	0.11
P	P2O5	24.47	0.15	0.83	Si	SiO2	5.45	0.21	0.22
Ca	CaO	6.28	0.05	0.27	P	P2O5	22.21	0.52	0.74
La	La2O3	9.85	0.1	0.14	Ca	CaO	1.26	0.08	0.05
Ce	Ce2O3	27.41	0.18	0.4	Fe	Fe2O3	1.75	0.19	0.05
Pr	Pr2O3	2.74	0.11	0.04	Y	Y2O3	0.08	0.37	0
Nd	Nd2O3	10.2	0.12	0.15	La	La2O3	9.87	0.35	0.14
Sm	Sm2O3	9.62	0.49	0.13	Ce	Ce2O3	25.57	0.64	0.37
Gd	Gd2O3	1.43	0.09	0.02	Pr	Pr2O3	2.53	0.38	0.04
Th	ThO2	4.69	0.09	0.04	Nd	Nd2O3	8.82	0.4	0.12
Total		100		2.15*	Sm	Sm2O3	11.18	1.77	0.15
					Gd	Gd2O3	1.13	0.34	0.01
					Tb	Tb2O3	0.07	0.35	0
					Dy	Dy2O3	0.41	0.33	0.01
					Ho	Ho2O3	0.07	0.3	0
					Th	ThO2	7.16	0.35	0.06
					Total		100		2.10*
			* Cation Sum						

Allanite

	Spectrum 1				Spectrum 25			
	Oxide	Oxide %	Oxide % Sigma	Number of Ions	Oxide	Oxide %	Oxide % Sigma	Number of Ions
O				12				12
Mg	MgO	0.13	0.33	0.02	Al	Al2O3	20.2	0.07	2.04
Al	Al2O3	13.65	0.09	1.47	Si	SiO2	32.43	0.09	2.77
Si	SiO2	30.09	0.09	2.76	Ca	CaO	11.72	0.04	1.07
Ca	CaO	10.65	0.04	1.05	Mn	MnO	1.02	0.05	0.07
Ti	TiO2	2.17	0.05	0.15	Fe	Fe2O3	11.18	0.07	0.72
Mn	MnO	0.29	0.05	0.02	Y	Y2O3	1.14	0.07	0.05
Fe	Fe2O3	14.81	0.08	1.02	La	La2O3	3.59	0.07	0.11
Y	Y2O3	0.49	0.07	0.02	Ce	Ce2O3	8.7	0.11	0.27
La	La2O3	3.58	0.1	0.12	Pr	Pr2O3	1.03	0.08	0.03
Ce	Ce2O3	10.11	0.12	0.34	Nd	Nd2O3	3.58	0.09	0.11
Pr	Pr2O3	1.11	0.09	0.04	Sm	Sm2O3	5.96	0.46	0.18
Nd	Nd2O3	4.21	0.1	0.14	Gd	Gd2O3	0.77	0.1	0.02
Sm	Sm2O3	6.03	0.52	0.19	Dy	Dy2O3	0.26	0.1	0.01
Eu	Eu2O3	0.08	0.1	0	Total		101.58		7.46*
Gd	Gd2O3	0.93	0.12	0.03					
Tb	Tb2O3	0.15	0.13	0					
Dy	Dy2O3	0.41	0.12	0.01					
Er	Er2O3	0.09	0.1	0					
Lu	Lu2O3	0.07	0.09	0					
Total		99.05		7.39*				* Cation Sum	

Xenotime

	Spectrum 23			
	Oxide	Oxide %	Oxide % Sigma	Number of Ions
O				4
Si	SiO2	1.42	0.07	0.05
P	P2O5	34.14	0.13	0.98
Fe	FeO	0.92	0.05	0.03
Y	Y2O3	38.66	0.16	0.7
Ce	Ce2O3	0.03	0.06	0
Nd	Nd2O3	0.44	0.06	0.01
Pm	Pm2O3	-0.13	0.07	0
Sm	Sm2O3	4.17	0.42	0.05
Gd	Gd2O3	2.43	0.08	0.03
Dy	Dy2O3	5.13	0.11	0.06
Ho	Ho2O3	1.34	0.11	0.01
Er	Er2O3	4.38	0.11	0.05
Tm	Tm2O3	0.44	0.11	0
Yb	Yb2O3	3.11	0.12	0.03
Lu	Lu2O3	0.44	0.11	0
Th	ThO2	0.97	0.09	0.01
U	UO2	1.31	0.08	0.01
Total		99.2		2.00*

Ilmenite

	Spectrum 22			
	Oxide	Oxide %	Oxide % Sigma	Number of Ions
O				3
Si	SiO2	0.16	0.03	0
K	K2O	0.07	0.01	0
Ti	TiO2	50.79	0.09	0.99
Mn	MnO	7.03	0.05	0.15
Fe	FeO	39.11	0.1	0.85
Nb	Nb2O5	0.47	0.05	0.01
Total		97.63		2.00*
			* Cation Sum	

Zircon

	Spectrum 24				Spectrum 18 (normalised)			
	Oxide	Oxide %	Oxide % Sigma	Number of Ions	Oxide	Oxide %	Oxide % Sigma	Number of Ions
O				4				4
Si	SiO2	30.85	0.09	0.98	Si	SiO2	32.06	0.13	0.99
K	K2O	0.12	0.02	0	Ca	CaO	0.42	0.02	0.01
Ca	CaO	0.24	0.02	0.01	Fe	FeO	0.63	0.04	0.02
Fe	FeO	0.38	0.04	0.01	Zr	ZrO2	65.9	0.21	0.99
Zr	ZrO2	64.35	0.18	1	Pr	Pr2O3	0.06	0.06	0
Sm	Sm2O3	0.47	0.38	0.01	Nd	Nd2O3	0.08	0.06	0
Eu	Eu2O3	0.08	0.07	0	Eu	Eu2O3	0.04	0.07	0
Gd	Gd2O3	0.11	0.09	0	Gd	Gd2O3	0.02	0.09	0
Tb	Tb2O3	0.12	0.09	0	Tb	Tb2O3	0.1	0.09	0
Dy	Dy2O3	0.09	0.09	0	Ho	Ho2O3	0.16	0.09	0
Ho	Ho2O3	0.1	0.09	0	Er	Er2O3	0.15	0.09	0
Er	Er2O3	0.11	0.09	0	Yb	Yb2O3	0.11	0.09	0
Tm	Tm2O3	0.08	0.09	0	Hf	HfO2	0.27	0.2	0
Yb	Yb2O3	0.14	0.09	0	Total		100		2.02*
Hf	HfO2	0.51	0.21	0					
U	UO2	0.19	0.07	0					
Total		97.93		2.02*				* Cation Sum	

Table 2. EDS analyses of target minerals.

4 Discussion and conclusions

Chemical and minero-petrographic analyses pointed out an enrichment in REEs (mostly Ce, La, Nd in monazite and allanite and Y in xenotime) in the magnetic fraction resulting from the industrial processing of the Montorfano granite. The results show that magnetic separation enhances the concentration of REEs minerals in the source rock. However, SEM-EDS-based automated analysis (AZtecFeature Suite) used for automatic identification of REEs-bearing minerals (Figure 5a) and particles/grain size revealed likely liberation issues preventing the effectiveness of the magnetic separation process; the average grain size of target minerals is extremely small compared to the associated gangue phases, although slight differences in size are noticeable between allanite, monazite, zircon, and ilmenite (Figure 5b).

Preliminary results of the work indicate that the major problem encountered lies in the limited particle liberation of REEs-bearing minerals, which are always locked within micas. It denotes that the particle size obtained by crushing and grinding the material before the magnetic separation process is too big to allow the liberation of monazite and other REEs minerals and their subsequent concentration in the following processing stages.

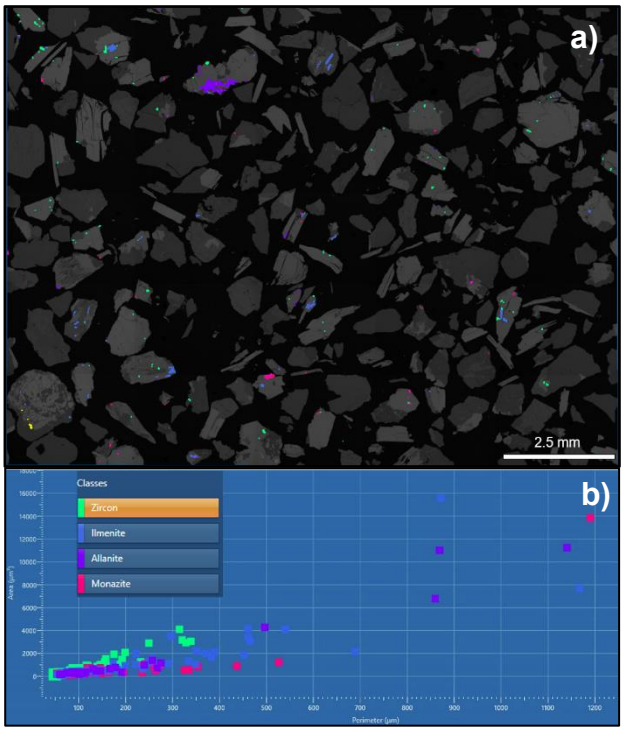

Figure 5. a Particle classification of ore minerals referring to the selected area of the SNG sample. **b** Binary diagram showing the correlation between grain size area (μm^2) and perimeter (μm) of target minerals.

Hence, an additional grinding step on the unprocessed material is probably required to achieve a roughly homogeneous grain size below 0.1 mm. This could make the particle liberation more effective, leading to a better concentration of ore minerals during magnetic separation and the possible consequent extraction of REEs metals through specific techniques.

In conclusion, the work assesses that the concentration of the REEs-bearing minerals in magnetic scraps from feldspar production, aiming at reusing such processing waste with economic benefits and reducing landfill volumes, is potentially feasible upon further concentration. Additional lab tests (i.e., hydrometallurgy tests on improved concentrated material) will confirm the viability of the recovery.

Acknowledgements

The work is part of the Ph.D. project “Exploration and recovery optimization of Critical Raw Materials for the green transition, toward zero-waste Circular Economy model” in the framework of “National Recovery and Resilience Plan (PNRR)”- PHD-Innovation 352.
The project is partially co-funded by Minerali Industriali S.r.l., which provides part of the facilities and equipment. The authors thank Minerali Industriali Engineering’s laboratory staff for their support during the sample preparation and analysis procedures.

References

Boriani, A., Bigioggero, B., and Origoni Giobbi, E. (1977). Geological map of the Verbania area; Memorie di Scienze Geologiche, vol. 32, fasc. 6.

Boriani, A., Burlini, L., Caironi, V., Giobbi Origoni, E., Sassi, A. N. G. E. U. C. A., and Sesana, E. L. E. N. A. (1988). Geological and petrological studies on the hercynian plutonism of Serie dei Laghi-geological map of its occurrence between Valsesia and Lago Maggiore (N-Italy); Rend. Soc. It. Mineral. Petrol, 43(367), 84.

Dino, G.A., Fornaro, M., and Trentin, A. (2012). Quarry waste: Chances of a possible economic and environmental valorisation of the Montorfano and Baveno granite disposal sites; Journal of Geological Research, 2012.

European Commission, 2020a. Critical materials for strategic technologies and sectors in the EU – a foresight study, 98 pp.

European Commission, 2020b. Critical Raw Materials Resilience: Charting a Path towards greater Security and Sustainability.

European Commission, 2020c. Study on the EU’s list of Critical Raw Materials – Final Report

Guastoni, A., Nestola, F., and Schiazza, M. (2017). Post-magmatic solid solutions of $CaCeAl_2(Fe^{3+}_{2/3\square 1/3})[Si_2O_7][SiO_4]O(OH)$, allanite-(Ce) and REE-bearing epidote in miarolitic pegmatites of Permian Baveno granite (Verbania, central-southern alps, Italy); Mineralogy and Petrology, v. 111, p. 315-323.